Electronic Supplementary Information

Facile formation of *meso–meso* linked porphyrin dimer catalyzed by a manganese(IV)–oxo porphyrin

Atsuro Takai,[a] Benoit Habermeyer[b] and Shunichi Fukuzumi*[a,c]

[a] *Department of Material and Life Science, Graduate School of Engineering, Osaka University and ALCA (JST), Suita, Osaka 565-0871, Japan*

[b] *ICMUB, UMR CNRS 5260, Université de Bourgogne, 9 Avenue Alain Savary, BP 47870, 21078 Dijon Cedex, France*

[c] *Department of Bioinspired Science, Ewha Womans University, Seoul 120-750, Korea*

Experimental

Materials. Zinc(II) 5,15-(*p*-tolyl)-10-(phenyl)porphyrin (ZnP), 5,10,15,20-tetrakis (2,4,6-trimethylphenyl) porphyrin (TMP), zinc(II) TMP (ZnTMP) were synthesized according to the literature.[1] (TMP)Mn^{III}(Cl) was obtained by adding $MnCl_2 \cdot 4H_2O$ to TMP.[2] Tris(2,2'-bipyridyl)ruthenium(III) hexafluorophosphate $[Ru(bpy)_3](PF_6)_3$ was prepared from tris(2,2'-bipyridyl)-ruthenium(II) chloride hexahydrate by the oxidation with PbO_2.[3] Ferrocene was purified by sublimation under vacuum.[4] *m*-Chloroperbenzoic acid (*m*-CPBA) was purified by washing with phosphate buffer (pH 7.4) and dried under reduced pressure.[4] Tetra-*n*-butylammonium hydroxide (TBAOH) 37% in methanol (Tokyo Chemical Industry Co., Ltd.), dichloromethane (CH_2Cl_2) and acetonitrile (MeCN) spectroscopic grade (Nacalai Tesque, Inc.) were obtained commercially and used without further purification.

General Procedure. UV–vis–NIR spectra were recorded on a Hewlett Packard 8453 diode array spectrophotometer using 2 mm or 1 cm cuvette. ^{1}H NMR spectra were recorded on a JEOL AL300 (300 MHz) spectrometer. Chemical shifts are expressed in ppm relative to chloroform (7.26 ppm). MALDI TOF–MS measurements were performed on a AXIMA-CFR (Shimadzu).

Electrochemical Measurements. Cyclic voltammetry (CV) and differential pulse voltammetry (DPV) were performed with a BAS 100W electrochemical analyzer in a deaerated solvent containing 0.10 M $TBAPF_6$ as a supporting electrolyte at 298 K. A conventional three-electrode cell was used with a platinum working electrode and a platinum wire as a counter electrode. The redox potentials were measured with respect to the $Ag/AgNO_3$ (1.0×10^{-2} M) reference electrode. The potential values (vs $Ag/AgNO_3$) can be converted to those vs ferrocene/ferrocenium.

Electron Paramagnetic Resonance (EPR) Measurements. The EPR spectra were measured at various temperatures with a JEOL X-band spectrometer (JES-RE1XE). The EPR spectra were recorded under nonsaturating microwave power conditions. The magnitude of the modulation was chosen to optimize the resolution and the signal-to-noise (*S*/*N*) ratio of the observed spectra. The *g* values were calibrated with an Mn^{2+} marker. The solutions containing porphyrins were deaerated by argon purging for 10 min prior to use.

Synthesis of *meso*–(ZnP)$_2$. To a 60 mL of CH_2Cl_2/MeCN (1:1) solution of 5-phenyl-10,20-di(*p*-tolyl)porphyrin (2.5 mg, 67 μM) and (TMP)Mn^{III} (0.48 mg, 18 μM) was added an MeCN solution of *m*-CPBA (72 μM) and stirred at room temperature for 50 seconds. Then, ferrocene (100 μM) was added to give orange-brown solution. The solvent was evaporated to dryness and the residue was purified by column chromatography (silica gel, CH_2Cl_2) and recrystallized from CH_2Cl_2/MeCN (1:9) to give *meso*–(ZnP)$_2$ (2.1 mg, 83%). ^{1}H NMR ($CDCl_3$): δ = 9.03 (d, J = 4.9 Hz, 4H, β), 9.01 (d, J = 4.9 Hz, 4H, β), 8.69 (d, J = 4.9 Hz, 4H, β), 8.30 (m, 4H, Ph), 8.11 (m, 12H, β, *p*-Tolyl), 7.80 (m, 6H, Ph), 7.47 (d, J = 8.5 Hz, 8H, *p*-Tolyl), 2.61 (s, 12H, Me) ppm; TOF–MS (MALDI): *m*/*z* calcd. for $C_{80}H_{54}N_8Zn_2$ (+H^+) 1259.3; found 1259.1; UV–vis (CH_2Cl_2): λ_{max} (ε, M^{-1} cm^{-1}) = 418 (2.24×10^5), 455 (2.26×10^5), 559 (4.77×10^4), 598 (5.80×10^3) nm.

References

(1) (*a*) J. S. Lindsey, I. C. Schreiman, H. C. Hsu, P. C. Kearney and A. M. Marguerettaz, *J. Org. Chem.* 1987, **52**, 827; (*b*) M. O. Senge, Y. M. Shaker, M. Pintea, C. Ryppa, S. S. Hatscher, A. Ryan and Y. Sergeeva, *Eur. J. Org. Chem.* 2010, 237.

(2) *The Porphyrin Handbook*, ed. K. M. Kadish, K. M. Smith and R. Guilard, Academic Press, San Diego, 2000.

(3) R. E. DeSimone and R. S. Drago, *J. Am. Chem. Soc.* 1970, **92**, 2343.

(4) W. L. F. Armarego and C. L. L. Chai, *Purification of Laboratory Chemicals*, 5th ed., Butterworth-Heinemann, Oxford, 2003.

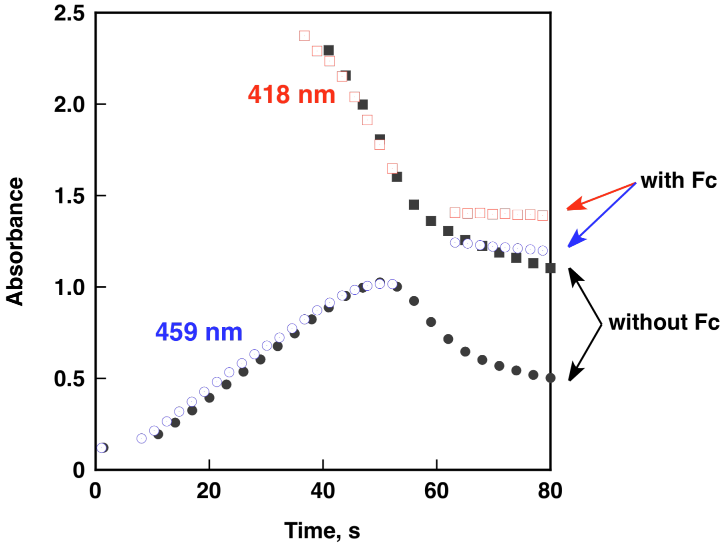

Fig. S1 Time profiles of the absorbance at 418 nm and 459 nm in the reaction of ZnP (6.7×10^{-5} M) with *m*-CPBA (1.3×10^{-4} M) in the presence of (TMP)Mn^{III}(Cl) (9.2×10^{-6} M) in CH_2Cl_2/MeCN (1:1 *v/v*) at 298 K.

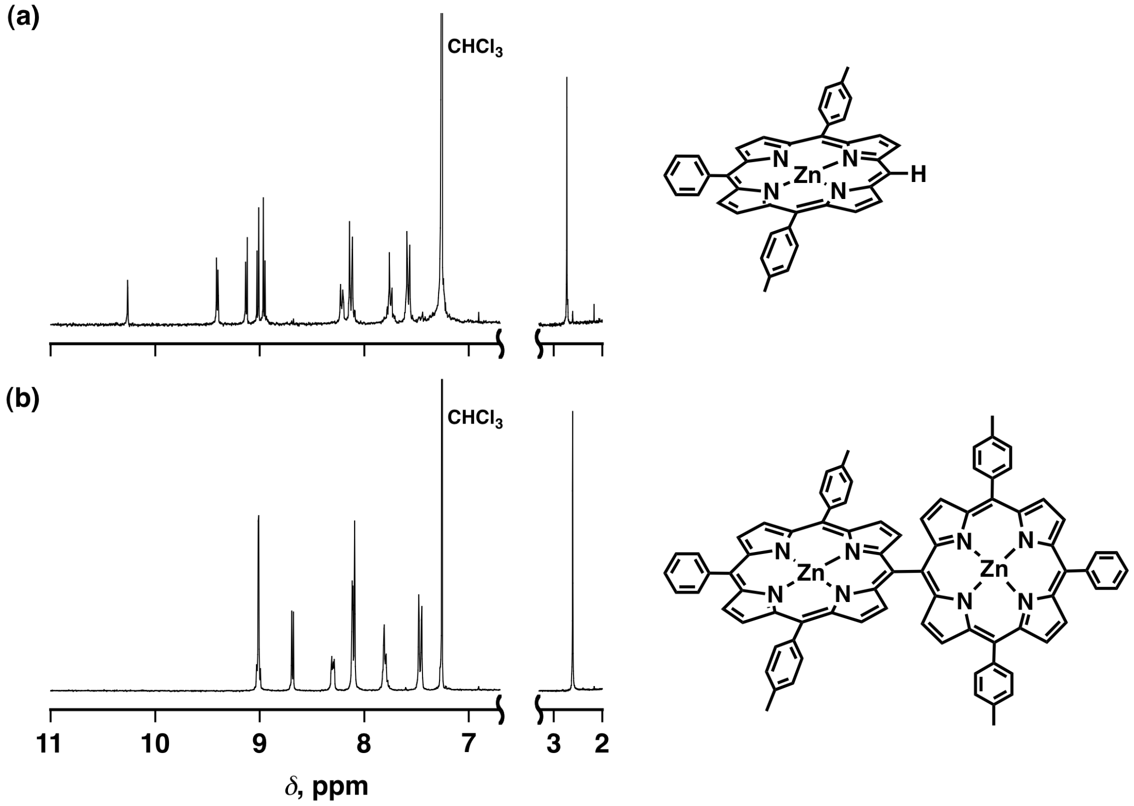

Fig. S2 ^{1}H NMR spectra of (a) ZnP and (b) *meso*–(ZnP)$_2$ obtained after silica gel column chromatography in $CDCl_3$ at 298 K.

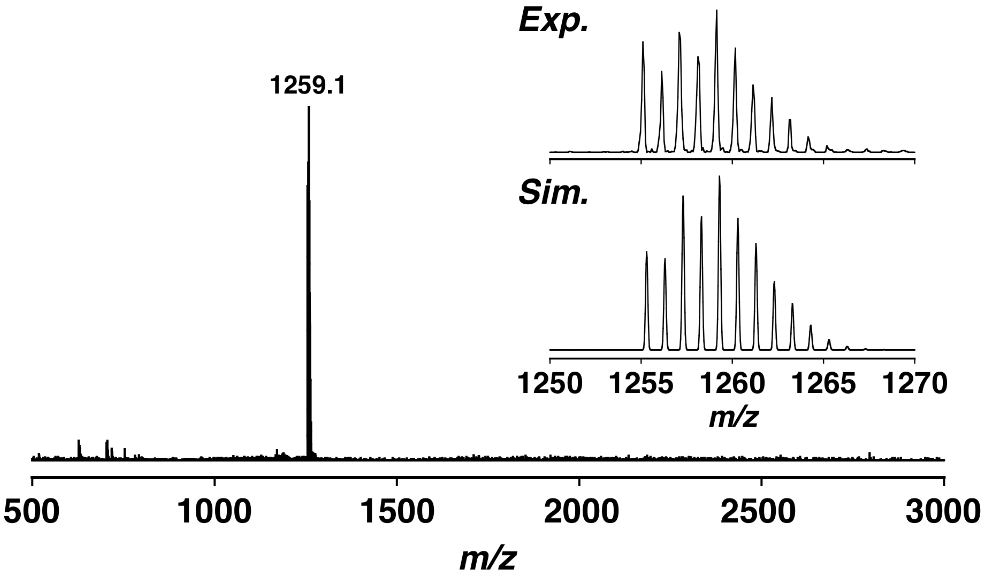

Fig. S3 MALDI TOF–MS of *meso*–(ZnP)$_2$, [M+H$^+$]. The calculated isotopic distribution for *meso*–(ZnP)$_2$ (*m*/*z* = 1259.3 calcd. for [M+H$^+$]) is shown in inset.

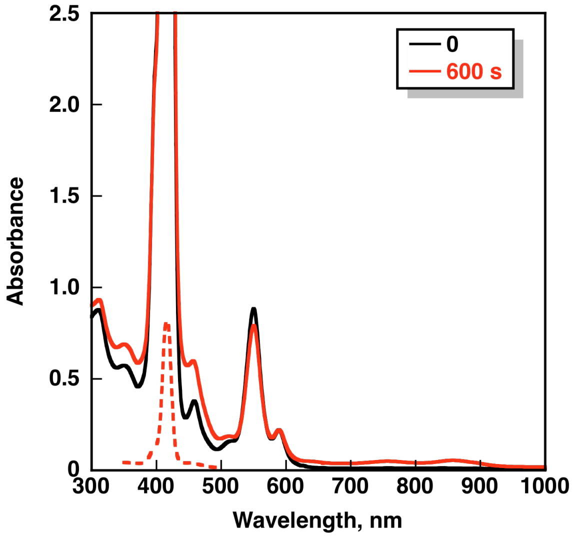

Fig. S4 UV–vis–NIR spectral change of ZnP (4.1×10^{-5} M) before and 600 seconds after the addition of *m*-CPBA (4.1×10^{-5} M).

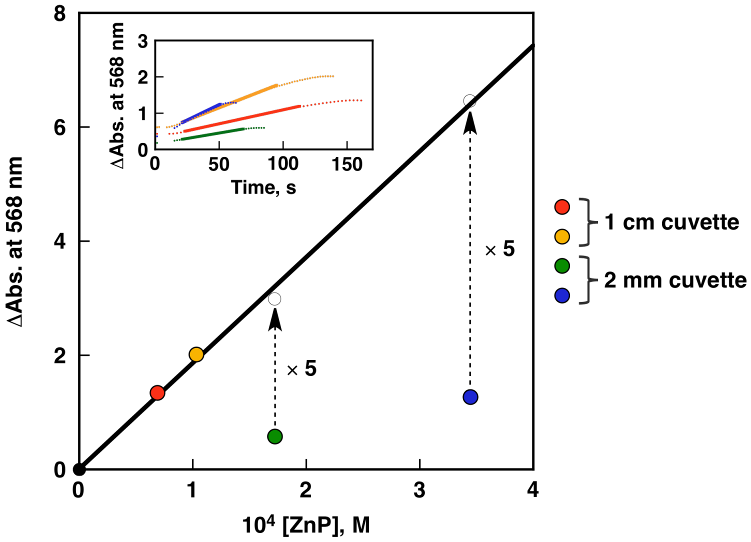

Fig. S5 Dependence of absorbance change (ΔAbs.) at 568 nm due to the formation of *meso*–(ZnP)$_2$ on [ZnP] in MeCN/CH$_2$Cl$_2$ (1:1). Inset: Time profiles of ΔAbs. at 568 nm in the reaction of [ZnP] and *m*-CPBA (1 equivalent to [ZnP]) in the presence of (TMP)Mn^{III}(Cl) (9.2 × 10^{-6} M).

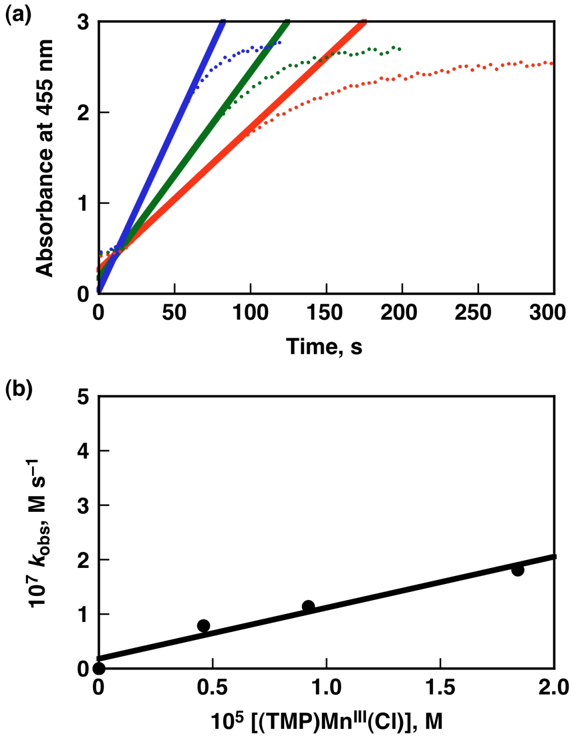

Fig. S6 (a) Time profiles of spectra in the reaction between ZnP (4.1×10^{-5} M) and (TMP)Mn^{III}(Cl) in the presence of *m*-CPBA (4.1×10^{-5} M) in MeCN/CH_2Cl_2 (1:1) at 298 K. (b) Dependence of the zero-order rate constant (k_{obs}) on [(TMP)Mn^{III}(Cl)].

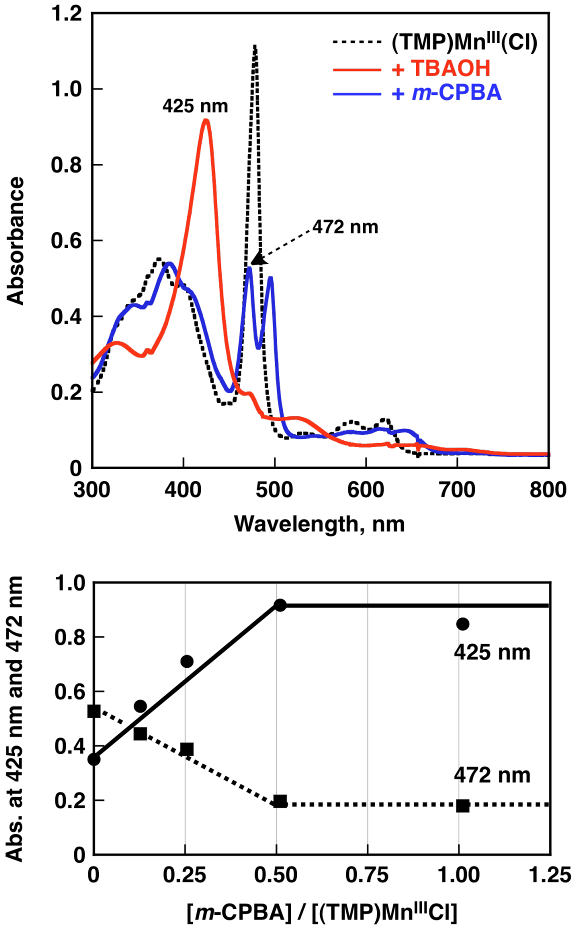

Fig. S7 (a) UV–vis spectra of (TMP)Mn^{III}(Cl) (dashed black line), (TMP)Mn^{III}(Cl) in the presence of 6 equivalents of TBAOH (blue line), and (TMP)Mn^{IV}(O) obtained upon addition of 0.5 equivalent of *m*-CPBA (red line) in MeCN/CH_2Cl_2 (1:1) at 298 K. (b) Plots of absorbance (Abs.) at 425 nm (solid line with circle) and 472 nm (dashed line with square) *vs.* [*m*-CPBA]/[(TMP)Mn^{III}(Cl)].

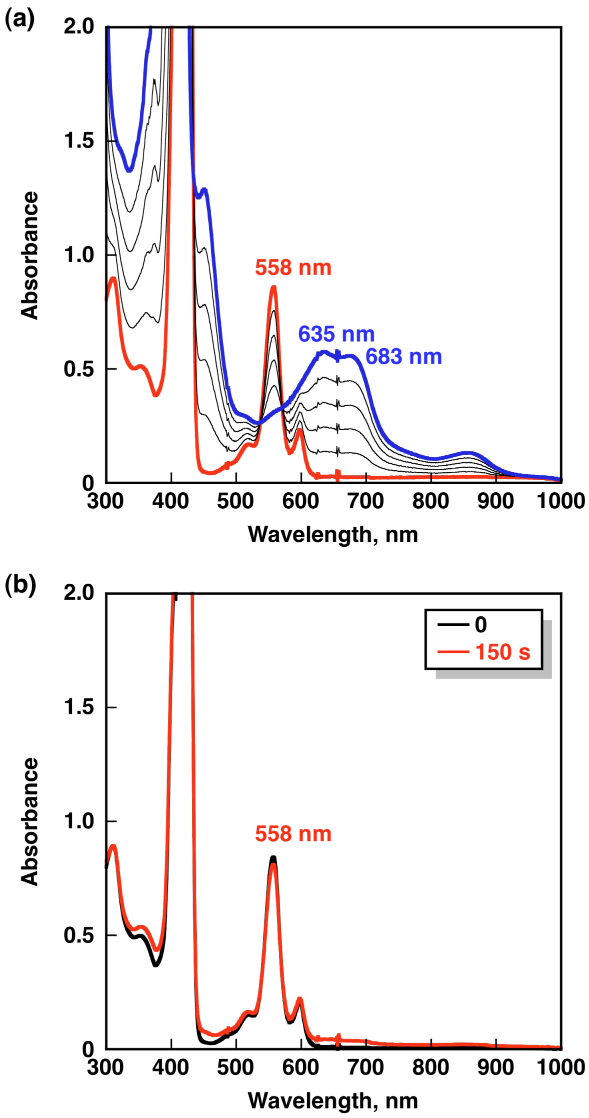

Fig. S8 (a) UV–vis–NIR spectral changes of ZnTMP (4.1×10^{-5} M) upon addition of $[Ru(bpy)_3]^{3+}$ (up to 1 equivalent) in CH_2Cl_2/MeCN (1:1) at 298 K. (b) UV–vis–NIR spectral change of ZnTMP (4.1×10^{-5} M) before and 150 seconds after addition of *m*-CPBA (1.6×10^{-4} M).

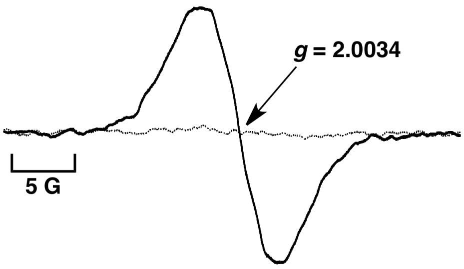

Fig. S9 EPR spectrum of ZnP (1.2×10^{-4} M) in the presence of (TMP)Mn^{III}(Cl) (3.5×10^{-5} M) 60 seconds after addition of *m*-CPBA (1.2×10^{-4} M) in CH_2Cl_2/MeCN (1:1) at 298 K (solid line). The dotted line indicates the EPR signal after addition of ferrocene.

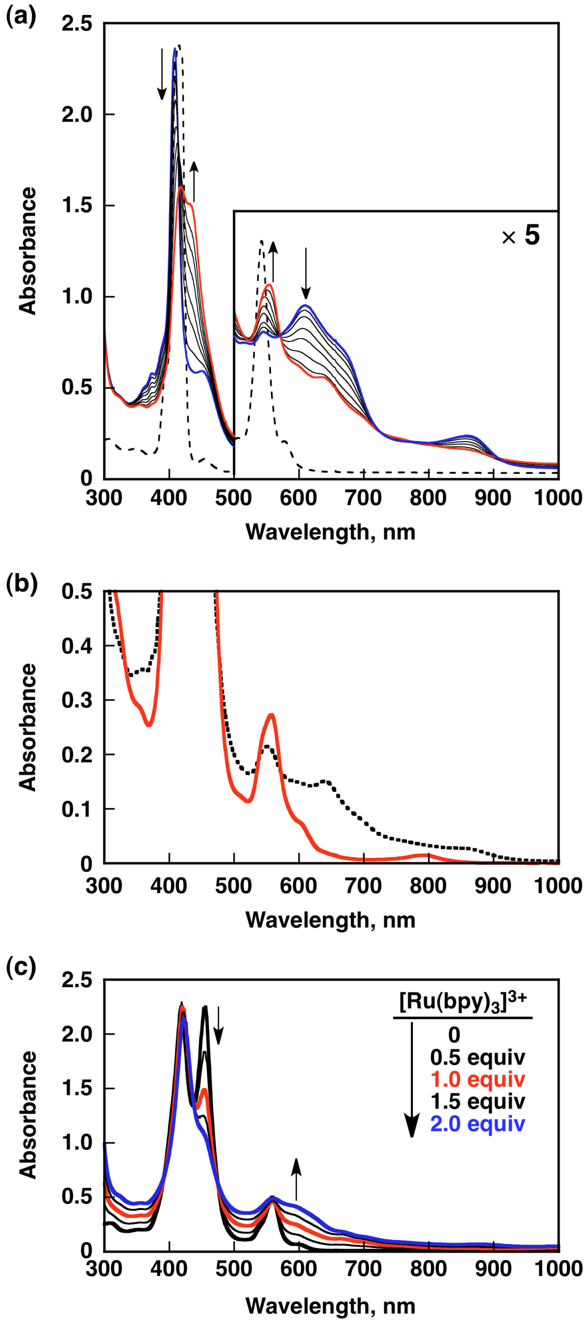

Fig. S10 (a) UV–vis–NIR spectral changes upon addition of 1 equivalent of $[Ru(bpy)_3]^{3+}$ to a CH_2Cl_2 solution of ZnP (6.9×10^{-5} M) at 298 K. (b) UV–vis–NIR spectral changes induced by addition of Fc. (c) UV–vis–NIR spectral changes of *meso*–$(ZnP)_2$ (1.0×10^{-5} M) upon addition of $[Ru(bpy)_3]^{3+}$ (0 to 2 equivalents) in CH_2Cl_2 at 298 K.

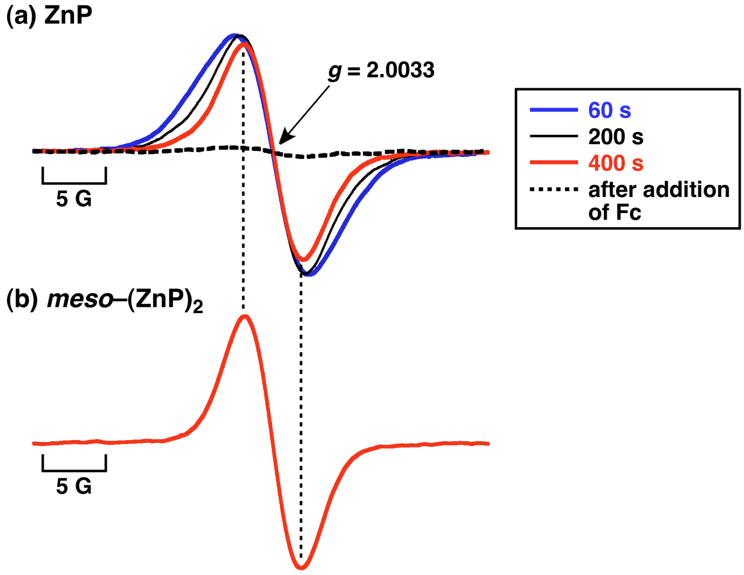

Fig. S11 (a) EPR spectral changes upon addition of 1 equivalent of $[Ru(bpy)_3]^{3+}$ to a CH_2Cl_2 solution of ZnP (2.5×10^{-4} M) at 298 K. (b) EPR spectrum of *meso*–$(ZnP)_2$ upon addition of 2 equivalents of $[Ru(bpy)_3]^{3+}$.